Ocean Engineering 44 (2012) 23–32

Contents lists available at SciVerse ScienceDirect

Ocean Engineering

journal homepage: www.elsevier.com/locate/oceaneng

Storm flooding sensitivity to sea level rise for Galveston Bay, Texas

Natalya N. Warner [a,*], Philippe E. Tissot [b]

[a] Department of Mathematics and Statistics, Texas A&M University–Corpus Christi, Corpus Christi, TX 78412, USA
[b] Conrad Blucher Institute, Texas A&M University–Corpus Christi, Corpus Christi, TX 78412, USA

ARTICLE INFO

Article history:
Received 24 June 2010
Accepted 2 January 2012
Editor-in-Chief: A.I. Incecik
Available online 14 February 2012

Keywords:
Coastal flooding
Exceedance probability of flooding
Galveston Bay
GEV probability distribution
Gulf of Mexico
Hurricane
Log-logistic probability distribution
Return period of flooding
Sea level rise
Surge

ABSTRACT

The combination of sea level rise and population growth in coastal regions makes it essential to continue improving flood management strategies. Flooding estimates must take into account both local vertical land motion and estimated rates of sea level rise linked to global climate change. Several extreme value distributions are compared using multiple statistical measures for the modeling of maximum annual storm surges based on the 105-year record of Galveston Pier 21, Texas. Increases in inundation frequencies are computed based on two possible sea level rise scenarios, a conservative linear continuation of the past century trend, and a scenario based on the upper limit of the sea level range in the IPCC AR4 report, i.e. the A1FI scenario. The research shows that by the year 2100 exceedance probabilities may double for the impact of the largest storms such as Hurricane Ike, but may increase by 6–7 times for the smaller surges associated locally with the impact of storms such as Hurricanes Cindy, Alicia, and Rita. While individually not as devastating or costly as large hurricanes, the cumulative and regular cost of smaller surge events could well be a bigger threat to coastal communities as sea level rises.

1. Introduction

Floods are the most common natural disasters that affect the United States. According to the United States Federal Emergency Management Agency (FEMA) almost 1.79 million properties were affected by floods from January 1978 to July 2011 in the United States with total monetary loss of approximately 39 billion dollars (NFIP, 2011). Floods have two major sources. River floods develop slowly and primarily impact communities in the vicinity of the streams, while floods generated by storm surges happen less frequently, more rapidly, and impact only coastal areas. Storm surge flooding can have a devastating impact on coastal locations, in some cases threatening the overall economic viability of coastal regions. Examples include the human and economic losses caused by recent events such as the Louisiana Flood in 1995, Hurricane Floyd in 1999, tropical storm Allison in 2001, Hurricanes Ivan in 2004, Katrina and Rita in 2005, Ike in 2008, and Irene in 2011.

Significant storms also generate large numbers of insurance claims placing unprepared insurance companies at risk. For example at least 11 insurance companies became insolvent after the passage of Hurricane Andrew in 1992 (Teugels and Sundt, 2004). More recently the landfall of Hurricane Ike in Galveston and other recent storms in Texas prompted the Texas legislature to update the state's windstorm insurance program (Ramsey, 2011). In addition, estimates for the rate of occurrence of storm surges and for the impact of storm surge flooding are important input in the establishment of governmental policies. For example, policies of the US National Flood Insurance Program are based on the occurrence rate and impact of future floods: "households with two flood-related claims are now required to be elevated by 2.5 cm above the 100-year flood level, or to relocate" (Bates et al., 2008). It is therefore of great interest to estimate as accurately as possible the rate at which storm surge flood events can be expected to occur and their likely impact (Beirlant et al., 2005).

Sea level rise, whether caused by downward vertical land motion or global sea level rise, will cause storm surge floods to progress further inland, thereby increasing flood damage and the recurrence interval of present 20- or 100-year floods. Recent research results indicate that effects of sea level rise on storm surge impact and occurrence rate estimates may not be adequately accounted for. Research by Purvis et al. (2008) examined the probability of future coastal flooding in the United Kingdom, given the uncertainty over possible sea level rise. They concluded that focusing only on the most plausible sea level rise may significantly underestimate monetary losses as it fails to account for the impact of low probability, high consequence events. Another study by Frazier et al. (2010) concludes that the impact of storm surges in Sarasota County, Florida, caused by small hurricanes will increase due to sea level rise.

A number of studies have been conducted to model flood resulting from river flooding and storm surges using a variety of extreme value distributions. The generalized extreme value (GEV)

* Corresponding author.
E-mail addresses: Natalya.Warner@tamucc.edu (N.N. Warner), ptissot@lighthouse.tamucc.edu (P.E. Tissot).

0029-8018/$ - see front matter © 2012 Elsevier Ltd. All rights reserved.
doi:10.1016/j.oceaneng.2012.01.011

distribution is recommended by FEMA (FEMA, 2007) and is the most widely used distribution in the field (Kotz and Nadarajah, 2000; Nadarajah and Shiau, 2005; ÖnÖz and Bayazit, 1995). However (Huang et al., 2008) suggested caution when applying the GEV after studying its application to locations along the East and Southeast Atlantic coast of the US and the Gulf of Mexico. Substantial differences between model and measurements were observed when comparing 100-year annual maximum water levels with historical data for these locations. While the modeled return periods exhibited less than 5% difference with observed data for locations along the Pacific and North East Coastal areas, a difference of over 21% was computed for Galveston Pier 21, Texas. Letetrel et al. (2010) used the generalized Pareto distribution to analyze the return periods of the sea level extremes in Marseille, France. Other distributions that have been used by prior researchers include the logistic and the log-logistic distribution (Ahmad et al., 1988; Rao and Hamed, 2000).

Ahmad et al. (1988) compared the log-logistic, GEV, three parameter log-normal and three parameter Pearson distributions. Datasets for their study were obtained for sites in Scotland with annual flood series varying in length from 5 to 66 years. The authors recommended "that the ideal distribution for flood frequency analysis should (a) reproduce at least as much variability in flood characteristics as observed in the empirical data sets; (b) be insensitive to extreme outliers especially in the upper tail; (c) must have a distribution function and an inverse distribution function that can be explicitly expressed in closed form; and (d) must not be computationally complex nor involve the estimation of a large number of parameters". For their study, the log-logistic distribution satisfied the above requirements better than other evaluated distributions. The goal of this study was to (1) identify the best performing distribution(s) for modeling extreme surges along the northern part of the Gulf of Mexico and (2) use the identified distribution to determine sensitivity of storm surge impact to sea level rise estimates. To this end, the study first compares performance of several distributions for the modeling of extreme surges at the US National Ocean Service station of Galveston Pier 21, Texas. This station was chosen because it has the longest water level record in the Gulf of Mexico starting in 1904 and because it is located in the economically important greater Houston area. The distribution that best models this data is then used to model future impact of storm surges for a broad range of storm sizes and for two distinct sea level rise scenarios.

2. Data and methods

2.1. Study site and data

The study site, the station of Galveston Pier 21 (Latitude 29°18.6′N, Longitude 94°47.6′W), is part of the US National Water Level Observation Network and is located on the north-east side of Galveston Island, Texas (Fig. 1).

The station is positioned on a ship channel about 4 km away from the main Galveston Ship Channel and the mouth of Galveston Bay. The station's records are available starting in January 1904 and include water levels measured hourly with only a few interruptions. This high quality 105 year time series is well suited for the comparison of statistical distributions of extreme events, and has been used for prior similar studies (Huang et al., 2008; Turner, 1991).

The 105 years of verified hourly water levels were obtained from NOAA's Tides and Currents data repository (NOAA, 2011a), and were further processed as follows. Monthly maximum water levels were obtained from the same site and compared to the maxima identified in the hourly time series. Most differences were within a range of 0.31 m, the station's Mean Range of Tide

Fig. 1. Map of the study area, the entrance of Galveston Bay, Texas. The study station is indicated by the red dot.

(NOAA, 2011b). Substantial differences of 0.45 m and 1.22 m were found for Hurricane #6 of August 1909 and Hurricane #2 of September 1919. For these two storms NOAA maximum water level records are based on water marks such as marks on buildings. The monthly tide gage records during these two storms are different likely because of unidentified equipment malfunction during these storms (personal communications with Chris Zervas, NOAA CO-OPS). As the hourly water levels are inconsistent with building marks and the damage caused by the storms, the maximum water levels taken from building marks were retained for this study, i.e. 2.07 m for September 1919 and 0.39 m for August 1909. The mean sea level trend of 6.39 mm/year (NOAA, 2011c) was removed from the hourly time series with the zero mean sea levels set for year 1999 to match tidal predictions (NOAA, 2011d). The harmonically predicted water levels were also obtained from (NOAA, 2011a). They were subtracted from water level series to remove tidal variability and to compute surges. The tidal component for the two cases described above (August 1909 & September 1919) was not removed as the timing of the maximum water levels could not be reliably identified. Overall missing data accounted for 2.35% of the hourly time series. Two gaps represented a significant portion of the missing data: 178 days from March through October 1984 and 120 days from February through May 1916. Neither of these periods was affected by significant storms. For months which did not include any data, data was imputed by the means of the maximum surges for the corresponding months. The maximum annual surges were then identified using the imputed data. The timing of the missing data did not coincide with hurricanes or tropical storms impacting the Texas coast with two exceptions, the category 4 Hurricane #2 of August 1915 and the category 1 Hurricane #1 of July 1943. Reliable water level data was not found for these two events. The extreme event distribution sensitivity to the absence of these two events will be addressed in a later section by computing the variability in the distribution parameters for a range of likely surges.

The resulting surge time series is presented in Fig. 2a and compared to the water level maxima time series (Fig. 2b) where the sea level rise is clearly discernable. The surge time series is the basis for the statistical analysis of this research.

2.2. Extreme value statistical distributions

The extreme value distributions selected for this study included the GEV recommended by (FEMA, 2007), the log-logistic recommended by (Ahmad et al., 1988), the Dagum, and the three and four-parameter Burr models recommended by (Kleiber and Kotz, 2003; Reiss and Thomas, 2007). While results are presented

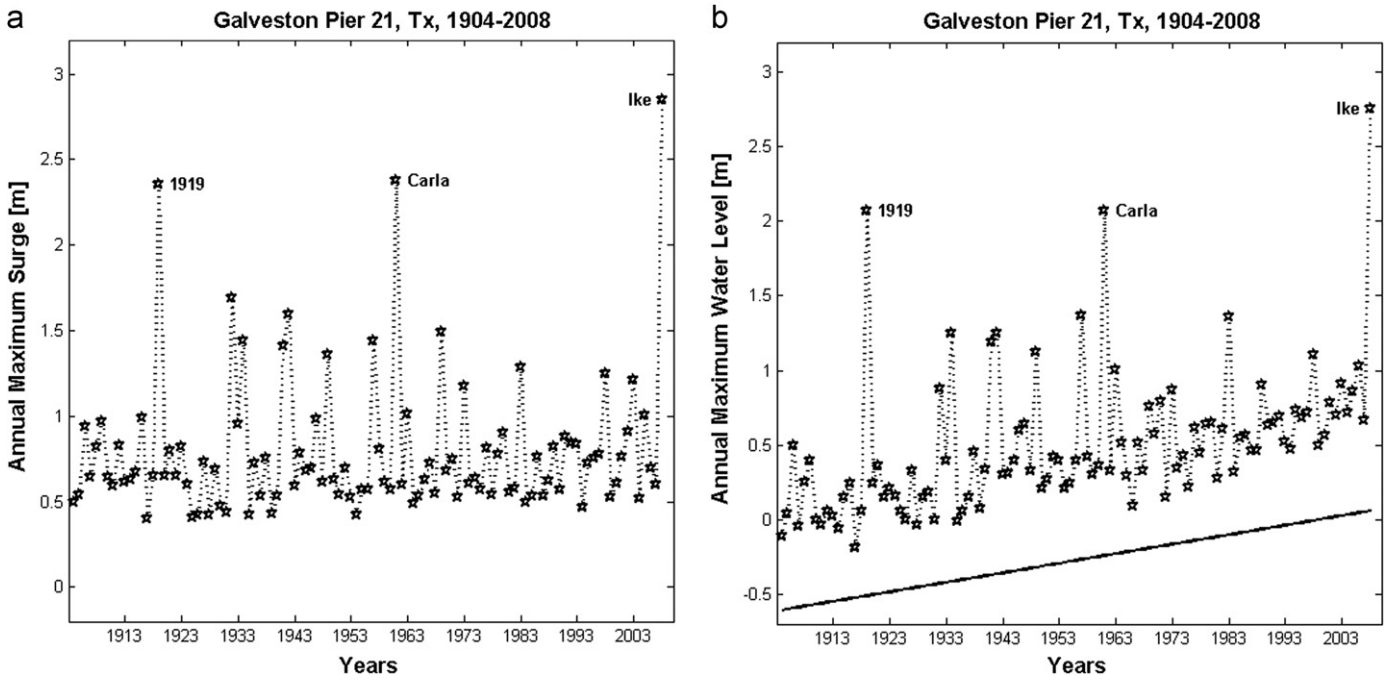

Fig. 2. (a) Annual maximum surge time series (b) annual maximum water level time series.

for these distributions, a number of other distributions available within the EasyFit Professional Software (EasyFit, 2004–2010) were compared including the Pearson, Wakeby, lognormal, Pareto, and other distributions. The selected distributions were both among the best performing based on the statistics below and were previously used to model riverine or storm surges.

Two goodness-of-fit tests were used to evaluate the suitability of the five selected probability distributions: the Kolmogorov–Smirnov (KS) and the Anderson–Darling (AD) tests. The statistic *Dn* of the KS test computes the maximum absolute value of the difference between the empirical and theoretical cumulative distribution functions over the relevant range of inputs. A smaller value of this statistic implies a better fit between the distributions (Rao and Hamed, 2000)

$$D_n = \max_x |F_n(x) - F(x)| \tag{1}$$

One of the AD tests is the *An* statistic. It is defined as the integral of the squared difference between the empirical and theoretical distribution functions multiplied by a weight function that emphasizes discrepancies in the tails. It is considered one of the most powerful tests for this type of distribution and can provide better discrimination between distributions and particularly their ability to model extreme events (ÖnÖz and Bayazit, 1995; Sinclair et al., 1990)

$$A_n^2 = n \int_{-\infty}^{\infty} \frac{(F_n(x) - F(x))^2}{F(x)[1 - F(x)]}\, dF \tag{2}$$

In the above expression n is the sample size, $F_n(x)$ is the empirical cumulative distribution function, and $F(x)$ is the theoretical cumulative distribution function. Sinclair et al. (1990) proposed a modified form of this test to emphasize the difference between the empirical distribution and theoretical distribution in one specific tail. One of the modifications of the test presented in their work, the AU_n statistic, gives a larger weight to the upper tail and is therefore well suited for our flood frequency analysis as the largest events have the biggest impact

$$AU_n^2 = n \int_{-\infty}^{\infty} \frac{(F_n(x) - F(x))^2}{[1 - F(x)]}\, dF \tag{3}$$

The following equivalent expression obtained after integration and simplification (Sinclair et al. (1990) was used for the AU_n statistic

$$AU_n^2 = \frac{n}{2} - 2\sum_{j=1}^{n} F(x(j)) - \sum_{j=1}^{n} \left[2 - \frac{(2j-1)}{n}\right] \log[1 - F(x(j))] \tag{4}$$

Again, a smaller value of this statistic implies a better fit between the distributions.

2.3. Rates of the sea level rise

Various studies (Bindoff et al., 2007; Domingues et al., 2008; Edwards, 2007; Gregory, 2008; Vermeer and Rahmstorf, 2009) indicate a large uncertainty in projections of the sea level rise by the end of the century. The difficulties in accurate estimation of sea level rise are due to uncertainty related to future changes in global atmospheric temperatures and still ongoing research on all possible contributions of melting ice sheets from Greenland and Antarctica (Gregory, 2008; Hansen, 2007; Meehl et al., 2007; Shum et al., 2008). For example the latest IPCC Fourth Assessment Report (AR4) (Meehl et al., 2007) projections likely do not include acceleration of future glacial contributions (Shum et al., 2008). While the higher end of the IPCC AR4 sea level rise estimates are used for this work, substantially higher sea level rise predictions can be found in recent work, e.g. in Vermeer and Rahmstorf (2009). Note that for the Gulf of Mexico only small regional deviations due to ocean density and circulation change relative to the global average sea level rise have been observed or predicted (Meehl et al., 2007) and such potential regional variability is not considered in this work.

For the purpose of this study, two sea level rise scenarios were selected:

- A very conservative continued linear sea level rise of 6.39 mm/yr, based on the 20th century trend for Galveston Pier 21 station (NOAA, 2011c), resulting in a 0.65 m increase in sea level by year 2100 as compared to 1999 mean sea level;
- A quadratic sea level rise rate, resulting in a total 1.08 m increase in sea level by year 2100 as compared to 1999 mean sea level. For this second scenario the local vertical land motion of 4.69 mm/yr was estimated by comparing last century's local

sea level rise rate (6.39 mm/yr) with a global sea level rise rate of 1.7 mm/yr (Bindoff et al., 2007). A quadratic sea level rise rate was then added to the vertical land motion rate to bridge the years between the last water level measurements and the global increase in sea levels as estimated for the A1FI 2090–2099 upper bound level (Meehl et al., 2007).

2.4. Analysis of the of the surge distribution for Galveston Pier 21

Water levels are driven by high frequency forcing, tidal, and meteorological, and by longer term factors such as local subsidence and global sea level rise (CCSP, 2009). For the study location these events are driven by meteorological forcing such as tropical and extra tropical storms with possible impact from precipitation and riverine input. While recent studies (Bender et al., 2010) suggest that climate change will modify both the overall frequency of tropical storms and the intensity distribution of storms in the Atlantic basin, records of past storm activity including recent events are yet to indicate any significant trend for the Atlantic Basin (Landsea, 2007) and Gulf of Mexico in particular (Levinson et al., 2010). Also, storm surge is not well correlated with the intensity of tropical storms. Estimates of changes in other storm characteristics such as size (Irish et al., 2008) and forward speed (Rego and Li, 2009) would have to be combined with possible changes in storm frequency to attempt estimates of changes in future storm surges. The meteorological forces driving storm surges, including the frequency and life cycle of tropical storms as well as the distribution of storm characteristics, are assumed stationary throughout the study period. To assess the validity of this assumption the parameters of each of the selected distributions were computed for a succession of 15 periods each 7 years long using the EasyFit Professional Software (EasyFit, 2004–2010). Monthly surge maxima rather than annual maxima were used for this test. While switching to monthly maxima increases the relative importance of smaller events the size of the data set is increased by an order of magnitude allowing for a more statistically robust assessment. The results of this fit are presented in Section 3 for the case of the log-logistic distribution.

3. Results

3.1. Stationarity of the surge distribution for station Galveston Pier 21, Texas

The stationarity of the surge time series was verified based on the monthly water level time series as described in Section 2.4. The parameters of the log-logistic distributions fitted for each of the 15 periods are presented in Fig. 3. The absence of significant trends supports the assumption of the stationarity of the surge distribution for the past century. For the past 105 years the only substantial difference in parameters is found for the 4th period (1925–1931) which can be explained by the smallest mean of the surge levels and the absence of hurricanes during that period. The results of this stationarity test were equivalent for the other distributions. The lack of trend for the distributions parameters also addresses the potential importance of increased mean water levels at the study location. Higher water levels in shallow bays should eventually lead to larger storm induced surges in the bays. The absence of impact from the mean sea level rise of 0.67 m from 1904 to 2008 is likely due in part to the proximity of the Pier 21 station to the Gulf of Mexico. The station is located on a ship channel about 4 km away from the main Galveston ship channel and near the mouth of Galveston Bay, a location for which sea level rise relative to water depth is much smaller than for the inland side or back bay of Galveston Bay.

3.2. Comparison of five extreme value distributions

The parameters for the five selected extreme value distributions were estimated and their cumulative distribution functions (CDF) compared against the empirical distribution using the 105 years maximum surge time series. The fitted values of the parameters for each distribution are presented in Table 1. Their goodness of fit as estimated by the KS statistic and the AD statistics with weights on both tails as well as the upper and lower tails alone are presented in Table 2. Comparisons of models using the same statistic are valid, but comparisons between two different statistics are not.

Comparing the results in Table 2, the three-parameter Burr distribution has the lowest statistics, i.e. the best performance

Table 1
Parameters for each of the 5 selected distributions.

	Shape	Shape	Scale	Location
Four-parameter Burr	**1.26**	**1.92**	**0.34**	**0.38**
Dagum	**0.59**	**2.35**	**0.39**	**0.39**
Three-parameter Burr	**0.27**	**10.19**	**0.52**	**–**
GEV	**0.35**	**–**	**0.17**	**0.60**
Log-logistic	**2.19**	**–**	**0.30**	**0.37**

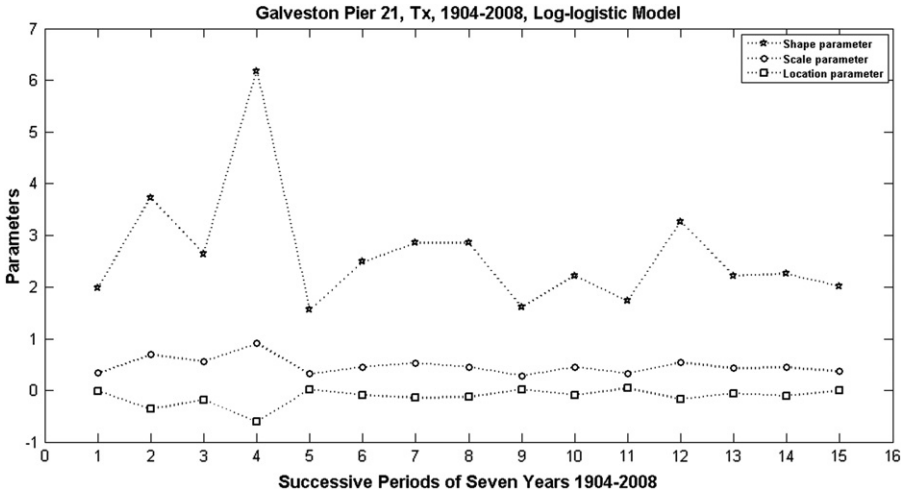

Fig. 3. Log-logistic distribution parameters computed on a series of monthly maxima (shape parameter is divided by 2).

for all measures, followed by the log-logistic, the GEV, the four-parameter Burr, and the Dagum distributions. The performance of the respective distributions is further evaluated graphically in Fig. 4 for the KS statistics, i.e. the absolute differences between the empirical and theoretical CDFs, for surges above 0.7 m. The largest discrepancy for this range of surge is observed around 0.85 m surges with differences in exceedance probabilities ranging from just below 0.03 for the three-parameter Burr to just below 0.04 for the four-parameter Burr distribution. For surges above 0.9 m the three-parameter Burr and log-logistic distributions perform slightly better than the other distributions.

To further compare the distributions, the related return periods are computed for surges of increasing size and the results compared to the return periods computed directly from the observed data, similar to the method used by Huang et al. (2008). The results are illustrated in Fig. 5. The observational return periods are computed by tallying the number of events up to a given surge without any smoothing contributing to the higher variability for long return period events. The difference between empirical and estimated return periods for the largest event in the data set, the surge generated by 2008 Hurricane Ike, are 1.2% for the log-logistic distribution, 2.5% for the three-parameter Burr, 5.4% for the four-parameter Burr, 7.6% for the Dagum Model, and 9.0% for the GEV model.

To test the robustness of the respective models the parameters of the distributions were recomputed for the first 104 years of the time series, omitting the 2008 surge generated by Ike (parameters are not shown in this publication). Return periods of 128, 146, 201, 176, and 212 years are obtained for the log-logistic, three-parameter Burr, four-parameter Burr, Dagum, and GEV distributions, respectively. The return period of 128 years estimated by the log-logistic distribution shows the best agreement with the 105 year return period from the historical time series.

An additional criterion for the selection of a distribution is its robustness to missing or potentially erroneous data. To estimate the sensitivity of the distributions to changes in the surges of large storms, the parameters of the distributions were recomputed for 15 alternate cases and compared to the original results. To create realistic alternate cases maximum water levels were replaced for one or more of the records for years 1909, 1915, 1919, and 1943. These four years were selected because their annual maxima were either based on building marks rather than water level measurements (1909 and 1919) or measurements during a hurricane were missing (1915 and 1943). For 1909 the second largest water level of 0.85 m was selected as an alternate value to 0.97 m. For the year 1919 the alternate value of 1.13 m was computed based on the historical hourly records instead of using the more realistic NOS monthly records and replaces 0.67 m. For years 1915 and 1943 the timing of the missing data coincides with the passage of major hurricanes, the category 4 Hurricane #2 of August 1915 and the category 1 Hurricane #1 of July 1943. For these years imputed data was used in the base line data set as described in Section 2.1. Alternate values for these two years were selected by computing the means of the surges for category 1 Hurricanes, 1.12 m, and for category 4 hurricanes, 1.78 m. These two water levels were used as alternate values for 2.35 m and 0.59 m in the baseline dataset.

Thus, the 15 alternate time series correspond to the 15 different ways of selecting one or more of the four alternate surges. For each distribution fitted to these alternate time series, exceedance probabilities were computed. The standard deviations of the 15 exceedance probabilities are compared graphically in Fig. 6. A lower standard deviation indicates a lower sensitivity to changes in single event values and is viewed as a positive characteristic of the distribution. For all distributions maximum sensitivity to changes in the data set is reached for surges just below 1 m. For maximum annual storm surges below 1.1 m the three-parameter Burr distribution shows the lowest standard deviation while for surges larger than 1 m the GEV shows the lowest standard deviation.

Table 2
Statistics of the KS test, AD test, and modified AD test for upper tail.

	Three-parameter Burr	Log-logistic	GEV	Four-parameter Burr	Dagum
KS statistic	**0.041**	**0.057**	**0.059**	**0.064**	**0.073**
AD upper statistic	**0.081**	**0.107**	**0.120**	**0.133**	**0.161**
AD normal statistic	**0.212**	**0.316**	**0.338**	**0.377**	**0.442**

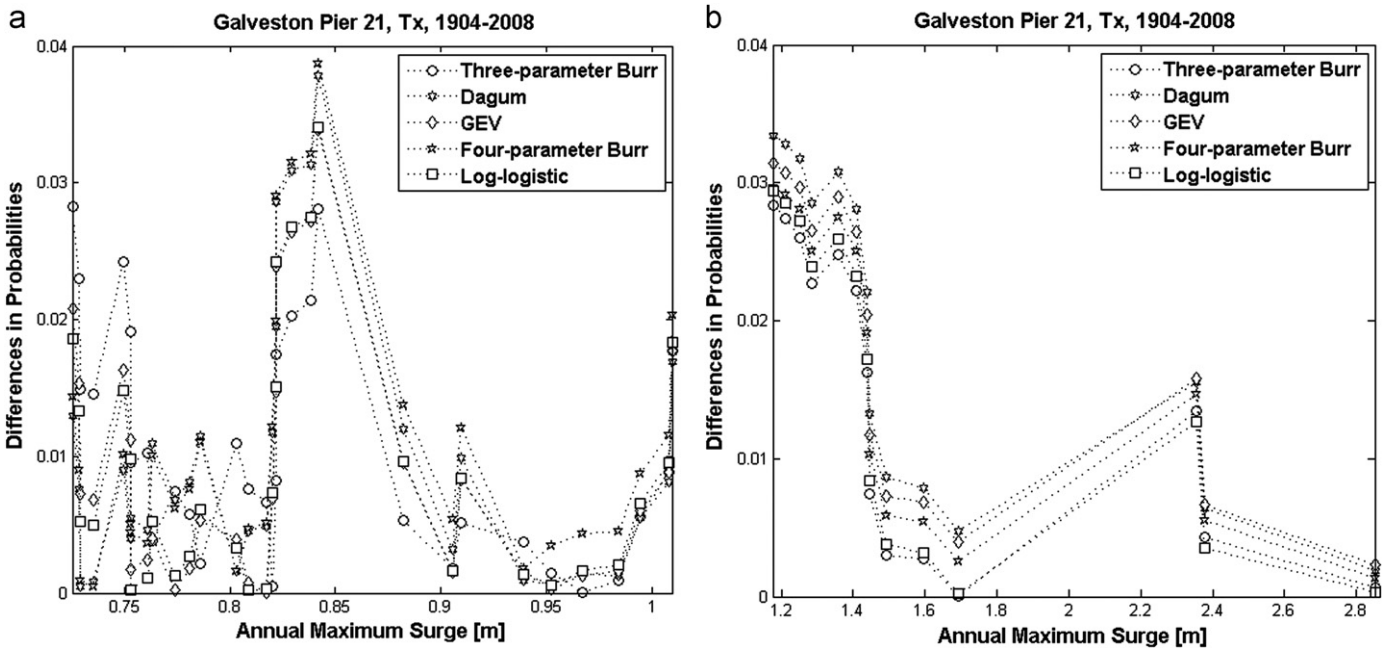

Fig. 4. Differences between the modeled and empirical CDFs as functions of surge for (a) 0.73–1.01 m surges and (b) 1.18–2.85 m surges.

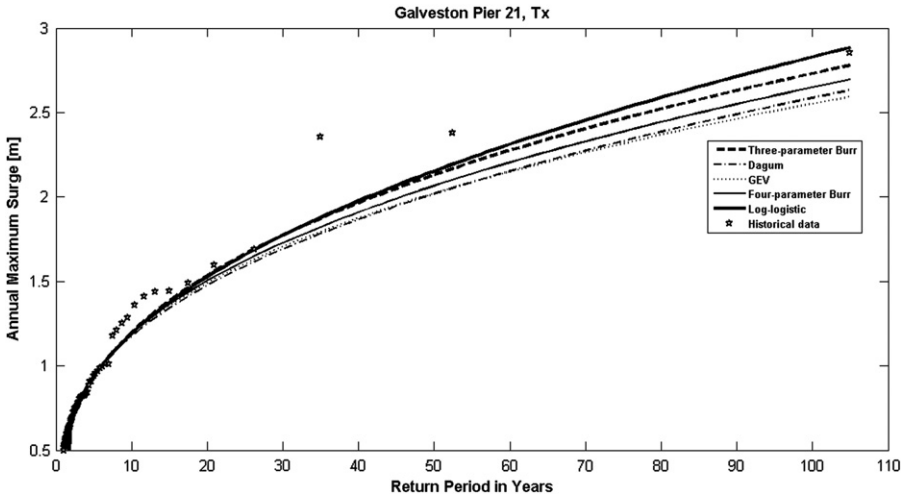

Fig. 5. Comparison of estimated return periods computed based on the observed data.

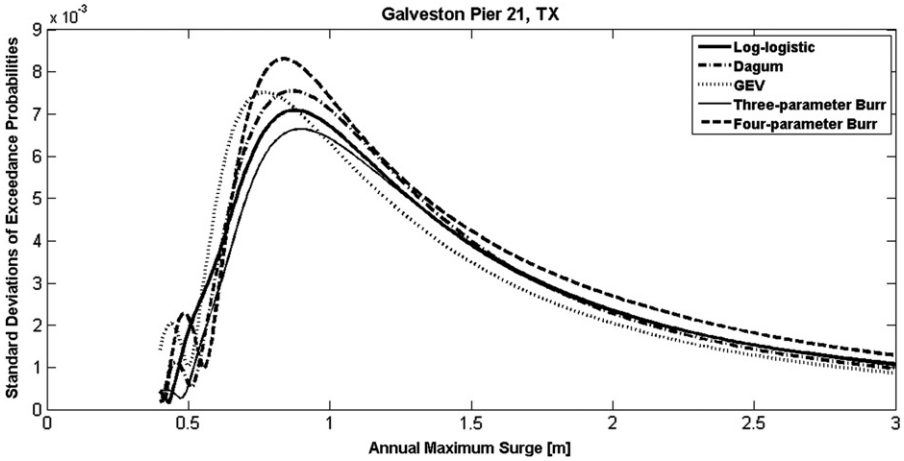

Fig. 6. Standard deviations of the exceedance probabilities for increasing surge levels when considering 16 cases to estimate the parameters of each model.

In Table 3 the performance of the respective distributions is evaluated by comparing modeled and observed surge exceedance probabilities for a wide range of significant events with surges above 0.9 m that impacted Galveston. All the distributions show a good agreement for surges up to 1 m. For the larger surges representing 10% or less of the record, a detailed comparison becomes more difficult due to the small number of large storms on record. In particular no events producing annual maximum surges between 1.69 m (1932 Hurricane #2) and 2.35 m (1919 Hurricane #2) have been recorded resulting in a step in the historical surge distribution. The five selected distributions have CDFs below the historical distribution for 1.2 m–1.4 m surges, then above the empirical distribution for surges between 1.6 m and 2.2 m. Agrement is good for the largest surges but the empirical distribution is based on only three storms for surges above 2 m: 2.35 m for 1919 Hurricane #2, 2.38 m for 1961 Hurricane Carla, and 2.85 m for 2008 Hurricane Ike. Overall the performance of the selected distributions for estimating return periods is quite similar with the largest discrepancies driven by the characteristics of the data set rather than by the features of the distributions.

Overall the small differences in performance between the five selected distributions do not lead to the outright exclusion of one or more of the distributions as a realistic description of the surge maxima. For the larger surges the performance of the log-logistic distribution is better than the other three distributions based on the AD test focused on the upper end of the distribution and the best for surges above 1.6 m based on the differences in CDF. While the three-parameter Burr had the best performance by some measures, we chose not to use it, because its performance was better for the lower surge events. Also, it is missing a location parameter which could make it more difficult to apply to other locations. When considering the robustness of the distributions the GEV distribution has the best performance for the larger surges although the differences are small. Because of the above results, the comparison of the KS and AD statistics, and for its ability to better model the return period of the large events, including the largest event in the data set, Hurricane Ike, the log-logistic distribution was selected for the rest of this study. The equation and parameters of the log-logistic CDF for this study are listed below following the convention by Kleiber and Kotz (2003):

$$F(x)=\left(1+\left(\frac{x-\gamma}{\beta}\right)^{-\alpha}\right)^{-1}, \quad \text{where } x>\gamma,\alpha>0,\beta>0,$$
$$\alpha=2.1893, \quad \beta=0.30158, \quad \gamma=0.36905 \tag{5}$$

3.3. Impact of sea level rise by 2100 for Galveston Pier 21, Texas

We use the fitted log-logistic maximum annual surge distribution to project inundation exceedance probabilities for future years while considering the two sea level rise scenarios described

Table 3
Comparison of modeled and observed surge exceedance probabilities listed in order of increasing maximum surge.

Hurricane or Tropical Storm	Year	Corresponding water level (m)	Annual max. surge (m)	CDF of historical data	Three-parameter Burr model	Log-logistic Model	GEV model	Four-parameter Burr Model	Dagum Model
Hurricane Allen	1980	0.65	0.91	0.78	0.78	0.78	0.78	0.78	0.78
Hurricane #5, 1933	1933	0.09	0.95	0.81	0.81	0.81	0.81	0.81	0.81
Hurricane #6, 1909	1909	0.39	0.97	0.82	0.82	0.82	0.82	0.81	0.82
Hurricane #3, 1947	1947	0.42	0.98	0.83	0.83	0.83	0.83	0.82	0.83
Hurricane #6, 1916	1916	0.24	0.99	0.84	0.83	0.83	0.83	0.83	0.83
Hurricane Rita	2005	0.86	1.01	0.85	0.84	0.84	0.84	0.84	0.84
TS Delia	1973	0.87	1.18	0.87	0.90	0.90	0.90	0.90	0.90
Hurricane Claudette	2003	0.91	1.21	0.88	0.90	0.90	0.91	0.91	0.91
TS Frances	1998	1.11	1.25	0.89	0.91	0.91	0.92	0.91	0.92
Hurricane Alicia	1983	1.36	1.28	0.90	0.92	0.92	0.92	0.92	0.92
Hurricane #10, 1949	1949	1.13	1.36	0.90	0.93	0.93	0.93	0.93	0.94
Hurricane #2, 1941	1941	1.19	1.41	0.91	0.94	0.94	0.94	0.94	0.94
Hurricane Audrey	1957	1.37	1.44	0.92	0.94	0.94	0.94	0.94	0.95
Hurricane #2, 1942	1942	1.25	1.59	0.95	0.96	0.96	0.96	0.96	0.96
Hurricane #2, 1932	1932	0.88	1.69	0.96	0.96	0.96	0.97	0.96	0.97
Hurricane #2, 1919	1919	2.07	2.35	0.97	0.98	0.98	0.99	0.99	0.99
Hurricane Carla	1961	2.07	2.38	0.98	0.99	0.98	0.99	0.99	0.99
Hurricane Ike	2008	2.76	2.85	0.99	0.99	0.99	0.99	0.99	0.99

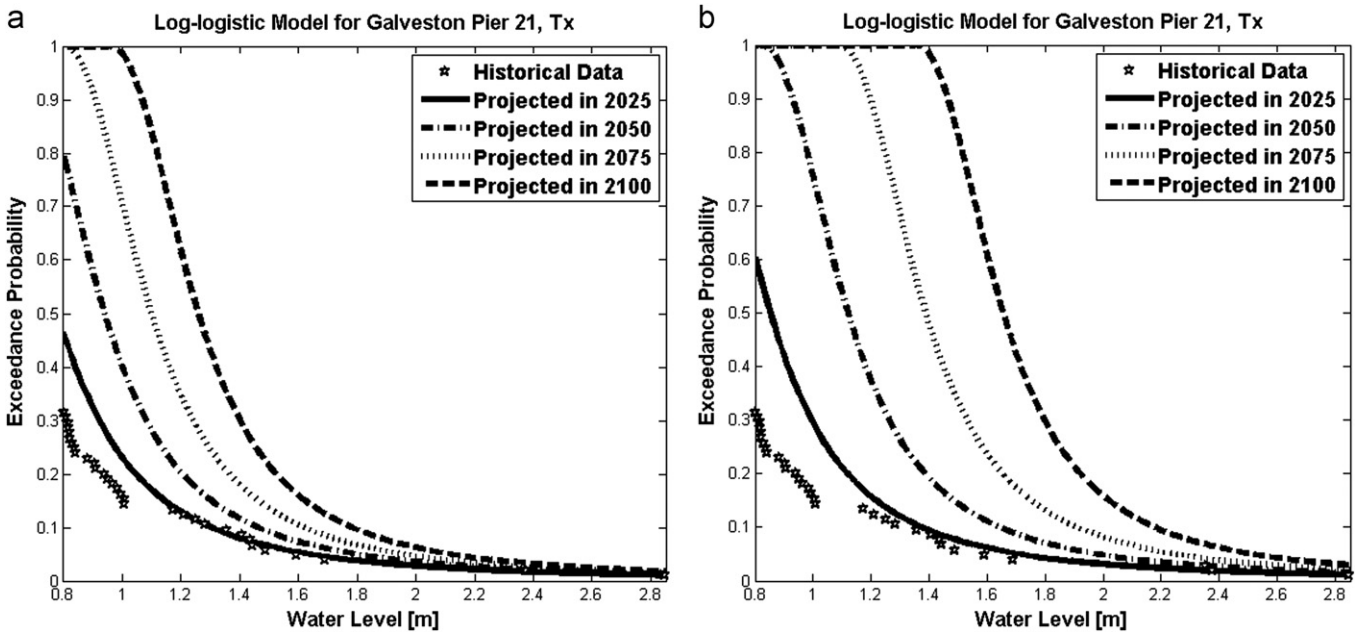

Fig. 7. Comparison of the projected water level exceedance probabilities for present water levels and including impact of two sea level rise scenarios (a) local sea level rise of 6.39 mm/yr and (b) a quadratic increase of the rate of sea level rise rate bases on IPCC AR4 scenario A1FI.

in Section 2.3. Exceedance probabilities are computed for both scenarios and compared in Fig. 7 for years 2025, 2050, 2075, and 2100. While all exceedance probabilities are rising, as expected, the changes are considerably more pronounced for small surge events. As an example, the sea level rise impact on the frequency of 1 m water level maximum, the local impact of 2005 Hurricane Rita, is considered. For the second sea level rise scenario the annual frequency of this event will increase presently from about 16% to 26% in 2025 and 62% in 2050. After year 2070 this type of event is predicted to take place every year. Even for the more conservative scenario, 1 m maximum water levels are expected to occur annually by year 2100.

The change of water level exceedance probability is further compared in Fig. 8 for the local impact of four storms: 2005 Rita (1.01 m surge), 1983 Alicia (1.28 m surge), 1957 Audrey (1.44 m surge), and 1942 Hurricane #2 (1.59 m surge). The frequency of the maximum annual water levels generated by Rita (1.01 m surge) increases much faster than that of the larger storms from 16% in 2008 to annually by 2100, more than a six fold increase, while for the 1.59 m surge case the frequency rises from about 4.5% to about 16%, more than a threefold increase. The faster rate of sea level rise of scenario 2 leads to substantially larger increases in water level exceedance frequency (Fig. 8b). For example, while for the 6.39 mm/yr sea level rise case the exceedance probability of the maximum water level generated by 1983 Alicia is predicted to be 45% in 2100, such an event is projected to take place annually for the faster rate of sea level rise case.

Fig. 9 displays the ratio of the water level exceedance probability in 2100 versus the present exceedance probability in 2009 for the conservative scenario. For relatively small events around 1 m, the ratio increases very rapidly due to the shape of the surge

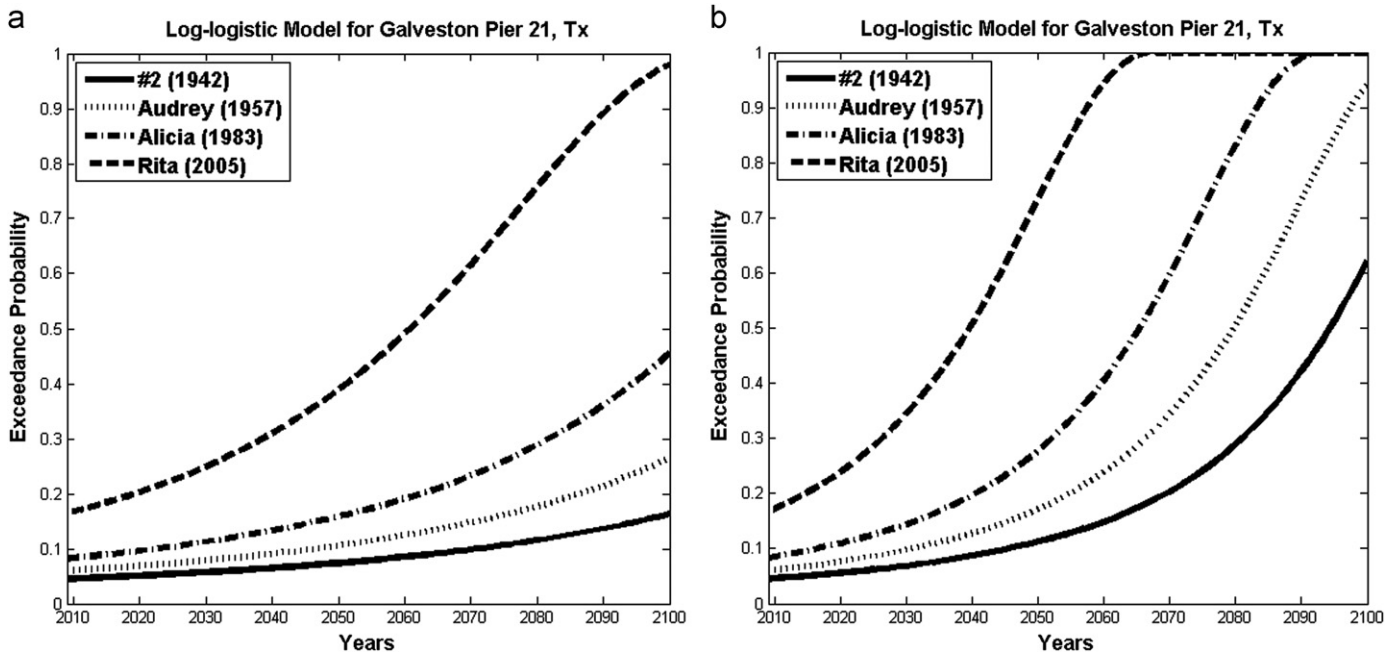

Fig. 8. Comparison of the increase in water level exceedance probabilities over the coming years for two sea level rise scenarios (a) local sea level rise of 6.39 mm/yr (b) a quadratic increase of the rate bases on IPCC AR4 scenario A1FI.

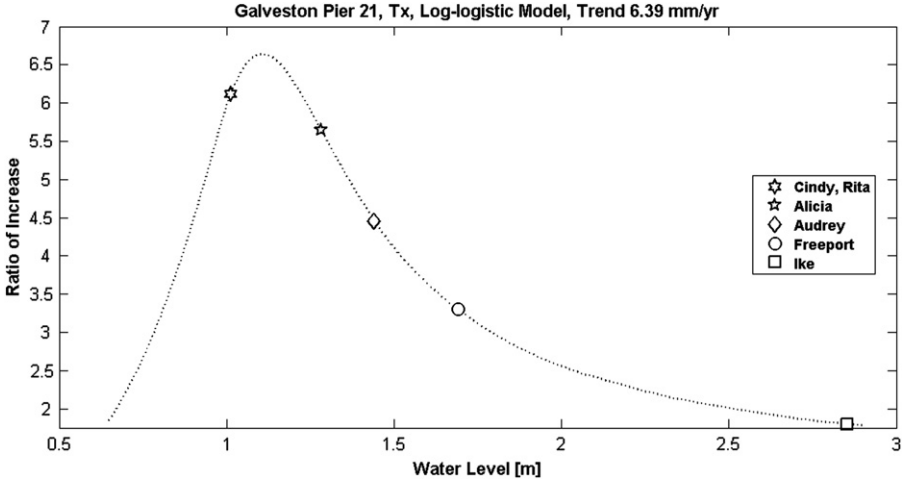

Fig. 9. Ratio of increase of projected exceedance probabilities in 2100 and 2008 for all water levels.

probability distribution. For events leading to smaller maximum water levels the increase is limited by a rapid rise to a 100% probability, i.e. the events are predicted to take place every year. The largest proportional increase is computed for a 1.1 m water level, which is predicted to occur 6.5 times as often in 2100. For events leading to larger surges, the relative exceedance probability ratio decreases progressively to about a factor 1.85 for the maximum water levels generated by 2008 Hurricane Ike. While a 1.85 times increase for such a large event is important given the damage caused by Ike (Report, 2008), this relative increase is considerably smaller than the 6.5 time increase for events generating a 1.1 m water level. This much larger projected increase in the frequency of the small to medium inundation events must be accounted for when projecting damage costs and insurance rates.

Finally, projected changes in return periods are computed up to year 2100 for a variety of storms that have impacted Galveston and for both scenarios the results are presented in Table 4. Return periods directly based on observations are listed under year 2008 while results for 2025, 2050, and 2100 are model based estimates. Differences in methodologies (more variability from the observational method) lead to the smaller estimated return periods for 2008 than for the 2025 and 2050 model estimates for two of the three largest surge events and for surges around 1.25 m. For the faster sea level rise scenario, by 2100 the maximum water level expected every year in Galveston is greater than the water levels of all but four hurricanes from the historical record, while the return period of an event of the magnitude of Hurricane Ike is predicted to decrease to 29 years from presently 105 years.

4. Conclusion

This study focused on quantifying the changing risks of flooding as the century progresses. The study started by comparing several extreme value distributions for estimating the probability of annual surge maxima for the station of Galveston Pier 21 in Galveston Bay,

Table 4
Projected return periods for inundation levels that have been generated by a range of historical storms for the study's two sea level rise scenarios.

Hurricane or Tropical Storm	Year	Month	Corresponding water level (m)	Annual max. surge (m)	Return period (in years) Log-logistic Model							
					Trend 6.39 mm/year				Quadratic increase of rate of SLR			
					in 2008	in 2025	in 2050	in 2075	in 2100	in 2025	in 2050	in 2075	in 2100
Hurricane Allen	1980	8	0.65	0.91	4.6	3.2	1.8	1.1	1.0	2.2	1.1	1.0	1.0
TS Fay	2002	9	0.70	0.91	4.8	3.2	1.8	1.1	1.0	2.2	1.1	1.0	1.0
	1906	10	0.50	0.94	5.0	3.5	2.0	1.2	1.0	2.5	1.1	1.0	1.0
Hurricane #5, 1933	1933	8	0.09	0.95	5.3	3.7	2.1	1.2	1.0	2.6	1.2	1.0	1.0
Hurricane #6, 1909	1909	8	0.39	0.97	5.5	3.9	2.2	1.3	1.0	2.7	1.2	1.0	1.0
Hurricane #3, 1947	1947	8	0.42	0.98	5.8	4.1	2.4	1.4	1.0	2.9	1.3	1.0	1.0
Hurricane #6, 1916	1916	8	0.24	0.99	6.2	4.3	2.4	1.4	1.0	3.0	1.3	1.0	1.0
Hurricane Rita	2005	9	0.86	1.01	6.6	4.5	2.6	1.5	1.0	3.1	1.3	1.0	1.0
Hurricane Cindy	1963	9	1.00	1.01	7.0	4.5	2.6	1.5	1.0	3.2	1.4	1.0	1.0
TS Delia	1973	9	0.87	1.18	7.5	7.3	4.6	2.6	1.5	5.4	2.4	1.0	1.0
Hurricane Claudette	2003	7	0.91	1.21	8.1	8.0	5.1	3.0	1.7	6.0	2.8	1.1	1.0
TS Frances	1998	9	1.11	1.25	8.8	8.9	5.7	3.5	1.9	6.7	3.2	1.2	1.0
Hurricane Alicia	1983	8	1.36	1.28	9.5	9.6	6.3	3.9	2.2	7.4	3.6	1.3	1.0
Hurricane #10, 1949	1949	10	1.13	1.36	10.5	11.4	7.7	4.9	2.9	8.9	4.5	1.6	1.0
Hurricane #2, 1941	1941	9	1.19	1.41	11.7	12.8	8.8	5.7	3.4	10.1	5.3	2.0	1.0
Hurricane Audrey	1957	6	1.37	1.44	13.1	13.6	9.5	6.2	3.8	10.8	5.8	2.2	1.0
Hurricane #3, 1934	1934	7	1.25	1.44	15.0	13.8	9.6	6.3	3.9	11.0	5.9	2.3	1.0
	1969	2	0.76	1.49	17.5	15.2	10.7	7.2	4.5	12.2	6.7	2.7	1.0
Hurricane #2, 1942	1942	8	1.25	1.59	21.0	18.5	13.5	9.4	6.2	15.2	8.8	3.8	1.2
Hurricane #2, 1932	1932	8	0.88	1.69	26.3	22.1	16.5	11.8	8.0	18.3	11.2	5.2	1.6
Hurricane #2, 1919	1919	9	2.07	2.35	35.0	55.8	46.1	37.3	29.6	49.5	36.1	23.3	11.9
Hurricane Carla	1961	9	2.07	2.38	52.5	57.3	47.4	38.5	30.6	50.9	37.2	24.1	12.5
Hurricane Ike	2008	9	2.76	2.85	105.0	93.1	79.9	67.8	57.0	84.3	66.2	47.6	29.5

Texas. The comparison focused on five frequently used distributions: GEV, log-logistic, three-parameter and four-parameter Burr, and Dagum. A comparative analysis of the distributions does not reveal significant differences in performance. The log-logistic distribution was selected to evaluate the probability of future flooding because of its good performance for the largest surges.

The study then uses the fitted log-logistic model to examine the effects of two forecasts of future sea level rises, a conservative scenario that continues the linear increase of the 20th century, and a scenario based on the upper end of the IPCC AR4 A1FI. Both scenarios show continuously increasing risks of flooding as the century progresses. By the end of the century, for the conservative scenario, inundations caused by the recent impact of Hurricane Rita are expected to take place annually, as compared to the current return period of 6.6 years. For the IPCC A1FI based scenario a Rita like flooding is expected to take place annually shortly after year 2050. The research shows differences in the relative increase in frequency of inundation caused by events of different sizes, and in particular a much larger proportional increase of flooding caused by smaller size storms. By year 2100 water level exceedance probabilities are expected to double for the impact of the largest storms such as Hurricane Ike, but increase by a factor over six times for the impact of smaller storm surges associated locally with the impact of storms such as Hurricanes Cindy, Alicia, and Rita for the conservative scenario. These results should be taken into account while estimating future insurance rates to cover the growing flooding damages as the century progresses.

Acknowledgments

The authors would like to thank Chris Zervas (NOAA National Ocean Service, Silver Spring, MD) for his help with the data set and other discussions. The authors also thank the valuable comments from Blair Sterba-Boatwright and Pablo Tarazaga of Texas A&M University–Corpus Christi, Texas.

References

Ahmad, M.I., Sinclair, C.D., Werritty, A., 1988. Log-logistic flood frequency analysis. J. Hydrol. 98 (3–4), 205–224.

Bates, B.C., Kundzewicz, Z.W., Wu, S., Palutikof, J.P., 2008. Climate Change and Water. Technical Paper of the Intergovernmental Panel on Climate Change. IPCC Secretariat, Geneva.

Beirlant, J., Goegebeur, Y., Teugels, J., Segers, J., 2005. Statistics of Extremes: Theory and Applications. John Wiley & Sons Ltd..

Bender, M.A., Knutson, T.R., Tuleya, R.E., Sirutis, J.J., Vecchi, G.A., Garner, S.T., Held, I.M., 2010. Modeled impact of anthropogenic warming on the frequency of intense Atlantic Hurricanes. Science 327 (5964), 454–458.

Bindoff, N.L., Willebrand, J., Artale, V., Cazenave, A., Gregory, J., Gulev, S., Hanawa, K., Le Quéré, C., Levitus, S., Nojiri, Y., Shum, C.K., Talley, L.D., Unnikrishnan, A., 2007. Observations: oceanic climate change and sea level. In: Solomon, S., Qin, D., Manning, M., Chen, Z., Marquis, M., Averyt, K.B., Tignor, M., Miller, H.L. (Eds.), Climate Change 2007: The Physical Science Basis. Contribution of Working Group I to the Fourth Assessment Report of the Intergovernmental Panel on Climate Change. Cambridge University Press, Cambridge, United Kingdom; New York, NY, USA.

CCSP, 2009. Coastal Sensitivity to Sea-Level Rise: A Focus on the Mid-Atlantic Region. A Report by the US Climate Change Science Program and the Subcommittee on Global Change Research. [James G. Titus (Coordinating Lead Author), K. Eric Anderson, Donald R. Cahoon, Dean B. Gesch, Stephen K. Gill, Benjamin T. Gutierrez, E. Robert Thieler, and S. Jeffress Williams (Lead Authors)]. Washington, DC, USA.

Domingues, C.M., Church, J.A., White, N.J., Gleckler, P.J., Wijffels, S.E., Barker, P.M., Dunn, J.R., 2008. Improved estimates of upper-ocean warming and multi-decadal sea-level rise. Nature 453 (7198), 1090–1093.

EasyFit, 2004–2010. Professional Software, 5.3 ed.. MathWave Technologies.

Edwards, R., 2007. Sea levels: resolution and uncertainty. Prog. Phys. Geogr. 31 (6), 621–632.

Frazier, T.G., Wood, N., Yarnal, B., Bauer, D.H., 2010. Influence of potential sea level rise on societal vulnerability to hurricane storm-surge hazards, Sarasota County, Florida. Appl. Geogra. 30 (4), 490–505.

Gregory, J.M., 2008. Sea level rise: what makes prediction so difficult? Planet Earth, Spring, 24–27.

Hansen, J.E., 2007. Scientific reticence and sea level rise. Environ. Res. Lett. 2 (024002). (6 pp).

Huang, W., Xu, S., Nnaji, S., 2008. Evaluation of GEV model for frequency analysis of annual maximum water levels in the coast of United States. Ocean Eng. 35 (11–12), 1132–1147.

Irish, J.L., Resio, D.T., Ratcliff, J.J., 2008. The influence of storm size on Hurricane surge. J. Phys. Oceanogr. 38 (9), 2003–2013.

Kleiber, C., Kotz, S., 2003. Statistical Size Distributions in Economics and Actuarial Sciences. Wiley and Sons.

Kotz, S., Nadarajah, S., 2000. Extreme Value Distributions: Theory and Applications. Imperial College Press, London.

Landsea, C., 2007. Counting Atlantic tropical cyclones back to 1900. Eos Trans. AGU 88, 18.

Letetrel, C., Marcos, M., Martín Míguez, B., Woppelmann, G., 2010. Sea level extremes in Marseille (NW Mediterranean) during 1885–2008. Cont. Shelf Res. 30 (12), 1267–1274.

Levinson, D.H., Vickery, P.J., Resio, D.T., 2010. A review of the climatological characteristics of landfalling Gulf hurricanes for wind, wave, and surge hazard estimation. Ocean Eng. 37 (1), 13–25.

Meehl, G.A., Stocker, T.F., Collins, W.D., Friedlingstein, P., Gaye, A.T., Gregory, J.M., Kitoh, A., Knutti, R., Murphy, J.M., Noda, A., Raper, S.C.B., Watterson, I.G., Weaver, A.J., Zhao, Z.-C., 2007. Global Climate Projections. In Climate Change 2007: The Physical Science Basis. Contribution of Working Group I to the Fourth Assessment Report of the Intergovernmental Panel on Climate Change. In: Solomon, S., Qin, D., Manning, M., Chen, Z., Marquis, M., Averyt, K.B., Tignor, M., Miller, H.L. (Eds.), Cambridge University Press, Cambridge, United Kingdom and New York, NY, USA.

Nadarajah, S., Shiau, J., 2005. Analysis of Extreme Flood Events for the Pachang River, Taiwan. Water Resour. Manage. 19 (4), 363–374.

NFIP, 2011. National Flood Insurance Program. Loss Statistics from January 1, 1978 Through Report as of 07/31/2011. 〈http://bsa.nfipstat.com/reports/1040.htm〉, (cited October 2011).

NOAA, 2011a. National Oceanic and Atmospheric Administration, Tides and Currents, Galveston Pier 21, TX. 〈http://www.co-ops.nos.noaa.gov/geo.shtml?location=8771450〉, (cited October 2011).

NOAA, 2011b. National Oceanic and Atmospheric Administration, Galveston Pier 21, Datums. 〈http://tidesandcurrents.noaa.gov/data_menu.shtml?unit=0&format=Apply+Change&stn=8771450+Galveston+Pier+21%2C+TX&type=Datums〉, (cited October 2011).

NOAA, 2011c. National Oceanic and Atmospheric Administration, Mean Sea Level Trend. 〈http://tidesandcurrents.noaa.gov/sltrends/sltrends_station.shtml?stnid=8771450+Galveston+Pier+21,+TX〉, (cited October 2011).

NOAA, 2011d. National Oceanic and Atmospheric Administration, Tidal Bench Marks. 〈http://www.co-ops.nos.noaa.gov/station_retrieve.shtml?type=Bench+Mark+Data+Sheets〉, (cited October 2011).

ÖnÖz, B., Bayazit, M., 1995. Best-fit distributions of largest available flood samples. J. Hydrol. 167 (1–4), 195–208.

Purvis, M.J., Bates, P.D., Hayes, C.M., 2008. A probabilistic methodology to estimate future coastal flood risk due to sea level rise. Coastal Eng. 55 (12), 1062–1073.

Ramsey, R., 2011. Lawmakers Approve Texas Windstorm Insurance Fix, The Texas Tribune. 〈http://www.texastribune.org/texas-legislature/82nd-legislative-session/lawmakers-approve-texas-windstorm-insurance-fix/〉.

Rao, A.R., Hamed, K.H., 2000. Flood Frequency Analysis. CRC Press, Inc..

Rego, J.L., Li, C., 2009. On the importance of the forward speed of hurricanes in storm surge forecasting: a numerical study. Geophys. Res. Lett. 36 (7), L07609.

Reiss, R.D., Thomas, M., 2007. Statistical Analysis of Extreme Values with Applications to Insurance, Finance, Hydrology and Other Fields, 3rd ed. Birkhäuser-Verlag, Basel–Boston–Berlin.

Report 2008. Hurricane Ike Impact Report. Foreword by Jack Colley. Chief, Texas Governor's Office of Homeland Security, Division of Emergency Management.

Shum, C.K., Kuo, C.-y., Guo, J.-y, 2008. Role of Antarctic ice mass balance in present-day sea-level change. Polar Sci. 2 (2), 149–161.

Sinclair, C.D., Spurr, B.D., Ahmad, M.I., 1990. Modified anderson darling test. Commun. Stat.—Theory Methods 19 (10), 3677–3686.

Teugels, J., Sundt, B., 2004. Encyclopedia of Actuarial Science. Wiley and Sons.

Turner, R., 1991. Tide gauge records, water level rise, and subsidence in the Northern Gulf of Mexico. Estuaries Coasts 14 (2), 139–147.

Vermeer, M., Rahmstorf, S., 2009. Global sea level linked to global temperature. Proc. Natl. Acad. Sci. 106, 21527–21532.